Accurate interband-Auger-recombination rates in silicon

D. B. Laks and G. F. Neumark
Division of Metallurgy and Materials Science, Columbia University, New York, New York 10027

S. T. Pantelides
IBM Research Division, Thomas J. Watson Research Center, P.O. Box 218, Yorktown Heights, New York 10598

(Received 26 February 1990)

Band-to-band Auger recombination is the dominant recombination mechanism in silicon at high carrier concentrations. Previous calculations found Auger rates too small to account for experiment. These calculations, however, contained uncontrolled approximations. We calculate accurate Auger recombination rates in both *n*-type and *p*-type silicon, avoiding approximations made in all prior Auger work. Our calculations show that Auger recombination is an order of magnitude stronger than previously thought. Our results for *n*-type Si agree well with experimental lifetimes. In contrast, a phonon-assisted mechanism is indicated for *p*-type Si. This conclusion can be understood based on details of the band structure.

INTRODUCTION

Electron and hole lifetimes are a key factor in semiconductor physics and technology. The study of these lifetimes is complicated by the variety of carrier-recombination mechanisms that determine them. Recombination mechanisms can be divided into two categories: defect and band to band. Defect recombination can be reduced by avoiding deep-level impurities that act as recombination centers. Band-to-band processes, which are present even in a perfect crystal, provide the ultimate limit to long lifetimes. The two main band-to-band recombination mechanisms are radiative and Auger recombination (AR). In AR an electron recombines with a hole and the energy of recombination is transferred to another electron or hole (Fig. 1).[1,2] In silicon and other indirect-band-gap semiconductors, where radiative recombination is inefficient, band-to-band AR dominates at high carrier concentrations. AR is important for technology as well: It competes with radiative recombination, reducing the efficiency of semiconductor lasers,[3] and it shortens the carrier diffusion lengths, reducing the efficiency of semiconductor solar cells.[4] By converting excess electron-hole pairs to excited carriers, AR plays a role in laser annealing of indirect-band-gap semiconductors.

Many authors have calculated Auger rates in a variety of semiconductors. Calculated Auger rates for silicon[5,6] (without phonon assistance) were an order of magnitude lower than experimental rates.[7,8] Because of this discrepancy, the observed recombination was attributed to a phonon-assisted mechanism, in which the carriers emit or absorb phonons during the Auger transition.[9,10] Calculations for silicon that included phonon-assisted transitions[11] were somewhat more successful in comparison with experiment. Careful examination, however, reveals potentially compromising approximations in *all* of these calculations (both with and without phonons). Examples include dropping a summation over the reciprocal lattice, and using model energy bands and wave functions. The validity of these approximations went untested.

In this paper we describe accurate calculations of the "pure" (no-phonon) Auger recombination rate in both *n*- and *p*-type silicon. We use accurate energy bands and wave functions and perform all summations until they are numerically converged. The Auger rate contains an eight-dimensional surface integral, which we evaluate over a cubic mesh. Furthermore, we have performed detailed convergence studies of all of the parameters that enter the calculation (e.g., the size of the mesh). This provides a quantitative measure of the accuracy of our results. Our theoretical recombination rates agree very well with experiment for heavily doped *n*-type silicon over the entire temperature range; theoretical rates for *p*-type silicon are much smaller than experiment. These

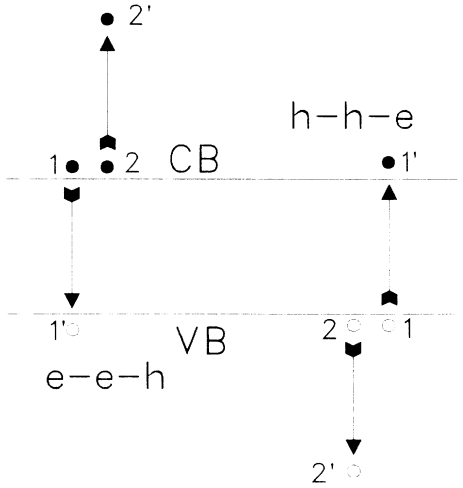

FIG. 1. *e-e-h* and *h-h-e* Auger recombination. CB and VB are conduction- and valence-band edges, respectively.

results suggest that pure AR is the dominant recombination mechanism in n-type Si, but that phonon-assisted recombination is in fact dominant in p-type Si. The band structure of silicon provides a simple explanation of this difference.

A brief summary of our results has been presented previously.[12,13] Here we give a detailed discussion of both our methods and results.

AUGER RATES AND THEIR MEASUREMENT

In this section we describe the relationship between Auger rates and lifetimes, and two of the experimental techniques used to measure them. This will provide a better understanding of the relation between the experimental and theoretical results.

Auger recombination involves either two electrons and a hole (electron-electron-hole, or *e-e-h* AR) or two holes and an electron (hole-hole-electron, or *h-h-e* AR). The interaction is mediated by the Coulomb repulsion between the like particles. The different AR mechanisms are characterized by nature of the electron and hole wave functions: in band-to-band AR, all particles are in the bulk bands; in defect AR, one or more particles are bound to crystal defects;[14] and in excitonic AR, the recombination is enhanced by the presence of electron-hole correlations.[15–17] In pure AR, the initial and final electronic states must conserve both energy and momentum. Momentum conservation can be relaxed by phonon emission or absorption (phonon-assisted AR) (Fig. 2). We have investigated the simplest of these processes—pure band-to-band AR.

The *e-e-h* Auger rate, R, is proportional to n^2p, where n and p are the electron and hole concentrations, respectively. [This is because an *e-e-h* Auger transition requires two electrons and a hole; the occupation probability for electrons (holes) is proportional to $n\,(p)$ using Boltzmann statistics.] Accordingly, the *e-e-h* Auger coefficient, C_n, is defined by $R=C_n n^2 p$. In heavily doped n-type silicon, where *e-e-h* AR is the dominant recombination mechanism, the hole lifetime is determined by $dp/dt=-R$. Using the definition of C_n, the hole lifetime is given by

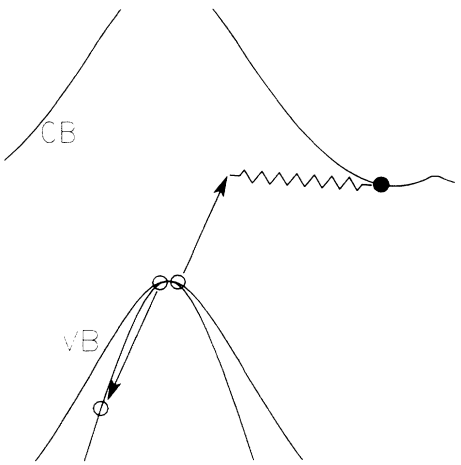

FIG. 2. Phonon-assisted Auger recombination.

$\tau^{-1}=R/p=C_n n^2$. The n^{-2} dependence of the hole lifetime is the hallmark of AR. (It is assumed here that the carriers are nondegenerate.) The relations for heavily doped p-type silicon, where *h-h-e* AR dominates, are completely parallel: the *h-h-e* Auger coefficient is defined by $R=C_p p^2 n$, and $\tau^{-1}=R/n=C_p p^2$. In the following, we will discuss the case of *e-e-h* recombination; *h-h-e* relations can be obtained by and interchanging the pairs (n,p) and (e,h).

The simplest way to determine Auger coefficients[7] is from measured carrier lifetimes [$C_n=(\tau n^2)^{-1}$]. The hole lifetime is measured as a function of electron concentration in a series of heavily doped n-type samples. Excess electron-hole pairs are created optically. After the excitation is removed, the hole lifetime is determined by monitoring the weak luminescence produced by the sample. The excited carrier concentration is much smaller that the dopant concentration, so that n remains constant during carrier recombination. In the region where AR is the dominant recombination mechanism, τ will be proportional to n^{-2}, and C_n will be given by the proportionality constant. This technique has two advantages. First, because the electron concentration is the equilibrium value, it can be measured easily, producing more accurate Auger rates. Second, C_n and C_p can be measured independently, by repeating the experiment with n-type and p-type materials. The one disadvantage of this method is that all measurements are made on heavily doped samples. Chemical impurities distort the band structure of doped material and the Auger rate may not be the same as for pure material.

The second technique measures the Auger rate in intrinsic material.[8] Here we have $n=p$, and the Auger rate becomes $R=(C_n+C_p)n^3$. As in the first method, excess electron-hole pairs are created by an external excitation, and luminescence is used to track the decay of the carrier concentration. With this method, however, the excess carrier concentration is no longer small compared to the equilibrium value. (AR is usually seen only for carrier concentrations much higher than the intrinsic values.) Hence, the total carrier concentration will decrease as a function of time during the luminescence decay. The Auger rate is determined by fitting $n\,(t)$ to the solution of the nonlinear differential equation

$$R=-dn/dt=(C_n+C_p)n^3+S(n)\ ,$$

where $S(n)$ is the rate for all other (significant) recombination processes. This method can only measure the combined Auger rate C_n+C_p. The technique is complicated, because of the need to measure excited carrier concentration, and to include all other significant recombination processes in $S(n)$. Fortunately, the Auger rates in silicon as measured by either method are in agreement. This demonstrates that heavy doping does not affect AR in silicon.

BASIC THEORY

In this section we will present the equations that are used in our theoretical calculations.

The total rate of pure AR is[18]

$$R=2\frac{2\pi}{\hbar}\frac{V^3}{(2\pi)^9}\int_{\mathrm{BZ}}\int_{\mathrm{BZ}}\int_{\mathrm{BZ}}\int_{\mathrm{BZ}}|M|^2 f(E_1)f(E_2)[1-f(E_{1'})][1-f(E_{2'})]$$
$$\times\delta(E_1+E_2-E_{1'}-E_{2'})\delta(\mathbf{k}_1+\mathbf{k}_2-\mathbf{k}_{1'}-\mathbf{k}_{2'})d\mathbf{k}_1\,d\mathbf{k}_2\,d\mathbf{k}_{1'}\,d\mathbf{k}_{2'}\ , \tag{1}$$

where $\mathbf{k}_1$, $\mathbf{k}_2$, $\mathbf{k}_{1'}$, and $\mathbf{k}_{2'}$ are the crystal momenta of the electrons and holes, and E_1, E_2, $E_{1'}$, and $E_{2'}$ are their energies (see Fig. 1). M is the Auger matrix element (see below), $\delta(E)$ and $\delta(\mathbf{k})$ are the energy- and momentum-conserving δ functions, and $f(E)$ is the probability that an electron is occupying the state with energy E. (For h-h-e AR, $f(E)$ is the occupation probability for a hole.) The k integrals span twelve dimensions; the momentum-conserving δ function can be used to eliminate the integration over $\mathbf{k}_2$, leaving a nine-dimensional integral. Contracting $\delta(E)$ reduces R to

$$R=2\frac{2\pi}{\hbar}\frac{V^3}{(2\pi)^9}\int_S\frac{|M|^2 f(E_1)f(E_2)[1-f(E_{1'})][1-f(E_{2'})]}{|\nabla_{\mathbf{k}}(E_1+E_2-E_{1'}-E_{2'})|}\ . \tag{2}$$

Here S is an eight-dimensional surface in $\mathbf{k}$ space defined by $E_1+E_2=E_{1'}+E_{2'}$ and $\mathbf{k}_1+\mathbf{k}_2=\mathbf{k}_{1'}+\mathbf{k}_{2'}$. The term in the denominator is the nine-dimensional gradient of $E_1+E_2-E_{1'}-E_{2'}$ with respect to $(\mathbf{k}_1,\mathbf{k}_2,\mathbf{k}_{1'})$.

The Auger matrix element is given by

$$M=\int\int\phi^*_{\mathbf{k}_1}(\mathbf{r}_1)\phi^*_{k_2}(\mathbf{r}_2)v(\mathbf{r}_1-\mathbf{r}_2)\phi_{\mathbf{k}_{1'}}(\mathbf{r}_1)\phi_{\mathbf{k}_{2'}}(\mathbf{r}_2)\mathrm{d}\mathbf{r}_1\,\mathrm{d}\mathbf{r}_2+\text{exchange term}\ ,$$
$$v(r)=\sum_{\mathbf{G}}\int_{\mathrm{BZ}}\frac{d\mathbf{q}}{(2\pi)^3}v(\mathbf{q}+\mathbf{G})e^{i(\mathbf{q}+\mathbf{G})\cdot\mathbf{r}}\ , \tag{3}$$

where $\phi_{\mathbf{k}}(\mathbf{r})$ is the wave function of the electron (or hole) with wave vector $\mathbf{k}$, $v(\mathbf{r})$ is the screened Coulomb potential,[19] and $\mathbf{G}$ is a reciprocal-lattice vector. The exchange term is found by changing $\phi_{\mathbf{k}_1}(\mathbf{r}_1)$ to $\phi_{\mathbf{k}_2}(\mathbf{r}_1)$ and $\phi_{\mathbf{k}_2}(\mathbf{r}_2)$ to $\phi_{\mathbf{k}_1}(\mathbf{r}_2)$. The q integration runs over the first Brillouin zone (BZ). $v(\mathbf{q}+\mathbf{G})$ is given by the product of the dielectric function and the Coulomb potential in reciprocal space:

$$v(\mathbf{q}+\mathbf{G})=\sum_{\mathbf{G}'}\epsilon^{-1}_{\mathbf{G},\mathbf{G}'}(\mathbf{q})\frac{4\pi e^2}{|\mathbf{q}+\mathbf{G}'|^2}\ , \tag{4}$$

where $\epsilon_{\mathbf{G}',\mathbf{G}'}(\mathbf{q})$ is the dielectric function of the material.[20] Using a diagonal approximation for ϵ^{-1} reduces $v(\mathbf{r})$ to

$$v(\mathbf{r})=\int\frac{d\mathbf{q}}{(2\pi)^3}\frac{4\pi e^2}{\epsilon(\mathbf{q})q^2}e^{i\mathbf{q}\cdot\mathbf{r}}\ , \tag{5}$$

where the integral now runs over all space.

Because of the periodicity of the crystal lattice, we can put the Auger matrix elements into a form that is easier to evaluate. The wave functions can be expanded in a Fourier series:

$$\phi_{\mathbf{k}}(\mathbf{r})=\frac{1}{\sqrt{V}}\sum_{\mathbf{G}}A(\mathbf{k}+\mathbf{G})e^{i(\mathbf{k}+\mathbf{G})\cdot\mathbf{r}}\ . \tag{6}$$

Using the Fourier expansion of all four wave functions and Eq. (5), the matrix element becomes

$$M=\frac{4\pi e^2}{V}\sum_{\mathbf{G}_1}\sum_{\mathbf{G}_2}\sum_{\mathbf{G}_{1'}}\sum_{\mathbf{G}_{2'}}A^*(\mathbf{k}_1+\mathbf{G}_1)A^*(\mathbf{k}_2+\mathbf{G}_2)B(\mathbf{k}_{1'}+\mathbf{G}_{1'})A(\mathbf{k}_{2'}+\mathbf{G}_{2'})$$
$$\times\frac{1}{|\mathbf{k}_{1'}+\mathbf{G}_{1'}-\mathbf{k}_1-\mathbf{G}_1|^2\epsilon(\mathbf{k}_{1'}+\mathbf{G}_{1'}-\mathbf{k}_1-\mathbf{G}_1)}+\text{exchange term}\ . \tag{7}$$

$\mathbf{G}_1$, $\mathbf{G}_2$, $\mathbf{G}_{1'}$, and $\mathbf{G}_{2'}$ are all reciprocal-lattice vectors. B is used to represent the Fourier components of the wave function with momentum $\mathbf{k}_{1'}$ to indicate that it is in a different band than the other wave functions. All other band indices are suppressed. Applying momentum conservation and substituting $\mathbf{G}=\mathbf{G}_1-\mathbf{G}_{1'}$ gives

$$M=\frac{4\pi e^2}{V}\sum_{\mathbf{G}}\frac{1}{\epsilon(\mathbf{k}_1-\mathbf{k}_{1'}+\mathbf{G})|\mathbf{k}_1-\mathbf{k}_{1'}+\mathbf{G}|^2}\sum_{\mathbf{G}_1}A^*(\mathbf{k}_1+\mathbf{G}_1)B(\mathbf{k}_{1'}+\mathbf{G}_1-\mathbf{G})$$
$$\times\sum_{\mathbf{G}_2}A^*(\mathbf{k}_2+\mathbf{G}_2)A(\mathbf{k}_1+\mathbf{k}_2-\mathbf{k}_{1'}+\mathbf{G}_2+\mathbf{G})+\text{exchange term}\ . \tag{8}$$

In this expression the summations over $\mathbf{G}_1$ and $\mathbf{G}_2$ are independent. As a result, the number of terms in each matrix element is reduced from N^3 to $2N^2$, where N is the number of reciprocal-lattice vectors used in the calculation. Note that because ϵ is a function of $\mathbf{k}+\mathbf{G}$, it cannot be factored from the $\mathbf{G}$ summation.

REVIEW OF PRIOR AUGER THEORY

Theoretical study of Auger recombination in semiconductors dates back to the pioneering work of Beattie and Landsberg.[1] In 1958 they investigated the rate of Auger recombination in InSb. To perform the integrals analytically, they made several major approximations in Eqs. (2) and (8). These approximations were designed for a narrow-band-gap direct-transition semiconductor (E_g $=0.18$ eV in InSb), where all of the $\mathbf{k}$ vectors are very near the band edge. During the last two decades these calculations were extended to other semiconductors, including Ge and Si,[5,6] GaAs[21-24] GaSb,[21] and InP.[23,24] Other authors calculated phonon-assisted Auger recombination rates in silicon,[11] and compound semiconductors.[15,25,26]

For silicon, Huldt[5] estimated the no-phonon Auger coefficient as $C_n=0.2\times10^{-31}$ cm^{6}sec^{-1} and predicted that C_p is much smaller than C_n, A later calculation by Hill and Landsberg[6] found $C_n=0.12\times10^{-31}$ cm^{6}sec^{-1}. On the experimental side, Dziewior and Schmid[7] deduced minority carrier lifetimes from luminescence decay in highly doped n-and p-type silicon at 77, 300, and 400 K. Their experimental Auger coefficients, $C_n=2.8\times10^{31}$ cm^{6}sec^{-1} and $C_p=0.99\times10^{-31}$ cm^{6}sec^{-1}, are much larger than the theoretical values. This led to the suggestion that phonon-assisted Auger recombination was responsible for the experimental rates.[9,10] Support for this thesis came from the temperature dependence of the Auger rate. The measured Auger rates $C(T)$ remain nearly unchanged in the temperature range $T=4$ to 400 K.[7,8] Huldt *et al.*[27] fitted these values to an expected analytical $C(T)$ for both no-phonon and phonon-assisted AR. With the given analytic forms a good fit could be made for the phonon-assisted case but not for the no-phonon case.[10] [The form used for phonon-assisted recombination was $C(T)=C_1\coth(\hbar\omega/2kT)$ where ω is the frequency of the phonon emitted during recombination. The form used for no-phonon AR was $C(T)$ $=C_2\sqrt{T}\exp(-E_{\rm Th}/kT)$ where $E_{\rm Th}$ is the threshold energy and is defined in the Results and Discussion section.] A subsequent calculation of the phonon-assisted Auger rate in silicon by Lochmann and Haug[11] found C_p in good agreement with experiment, but C_n was still four times too small. They concluded that phonon-assisted AR, not pure AR, is the dominant recombination mechanism in highly doped silicon. This conclusion was extended to other indirect-band-gap semiconductors as well.[11]

Careful examination shows that all existing Auger rate calculations—for both pure and phonon-assisted mechanisms and for any of the materials studied—retained many of the approximations of the original Beattie and Landsberg work,[1] even though they were never tested. The underlying assumptions of Beattie and Landsberg's approximations is that all of the $\mathbf{k}$ vectors in Eqs. (2) and (8) will be near the band edge, which is true only for a small direct band gap. These approximations may not be valid for wide band gap or indirect-transition semiconductors, where $\mathbf{k}_{2'}$ will be far from the band edge.

Before discussing the particulars of the approximations, it should be noted that there are two categories of theoretical papers under discussion. The difficulty of evaluating the quantities in Eqs. (2) and (8) has been met using two strategies. The first strategy is to introduce as many approximations as are needed to determine the Auger rate. This is the approach used by most authors. The second strategy is to give up on evaluating the full Auger rate in Eq. (2) and concentrate instead on determining the Auger matrix elements alone [Eq. (8)] using fewer approximations.[21-24,28] Approximations used in papers in the first category include the following

In the integration over $\mathbf{k}$ [Eq. (2)]:

(1) Of the eight dimensions in the $\mathbf{k}$-space integral, the matrix elements are integrated over, at most, six dimensions. (The reduction occurs because of other approximations, not all mentioned here, that are made.)

(2) Model ($\mathbf{k}\cdot\mathbf{p}$ or parabolic) band structures are used to find the energy conservation surface.

In the matrix element calculation [Eq. (8)]:

(3) The first summation over the reciprocal-lattice vectors ($\mathbf{G}$) is dropped. This approximation is often called neglecting "umklapp terms."

(4) The electron and hole wave functions are taken from $\mathbf{k}\cdot\mathbf{p}$ perturbation theory.

(5) The dielectric function, ϵ, which is in fact a function of $\mathbf{k}$, is either replaced by the static dielectric constant, ϵ_0, or left out entirely.

(6) Some authors do not calculate both the direct and the exchange terms of the matrix elements.

The papers that evaluate only the matrix elements make fewer approximations in Eq. (8). In particular, Brand and Abram[22] appear to be the only authors before this work to include both the sum over $\mathbf{G}$ and k dependence of ϵ. (They also use an empirical pseudopotential for the wave functions.) But, as noted above, these calculations are done for only a few matrix elements. As a result, these papers do not provide any estimate of the rate of Auger recombination, which is the quantity of interest. Of the previous evaluations of the total Auger rate, Beattie's work on InSb (Ref. 29) is probably the most accurate. Beattie used the Monte Carlo method to integrate the matrix elements over a full six dimensions in $\mathbf{k}$ space. The use of $\mathbf{k}\cdot\mathbf{p}$ band structure and wave functions, a static dielectric constant, and the omission of the sum over $\mathbf{G}$ are all appropriate for $\mathbf{k}$ vectors very near the band edge. These approximations may be adequate for InSb, where $\mathbf{k}_1$, $\mathbf{k}_2$, $\mathbf{k}_{1'}$, and $\mathbf{k}_{2'}$ are all near the band edge.

DESCRIPTION OF PRESENT WORK

We have performed a thorough calculation of the rate of pure *e-e-h* and *h-h-e* Ar in silicon. We do not use any approximations of unknown consequence; in particular all of the approximations described in the previous sec-

tion are avoided. In addition we have verified the accuracy of our numerical approximations through extensive convergence studies.

For the band structure [in Eq. (2)] and the wave functions [in Eq. (8)] we use empirical pseudopotentials.[30] (Nonlocal corrections and spin-orbit splitting were not included; both of these produce very small corrections to the bands that contribute to the total AR rate.) We chose an empirical potential over a first-principles pseudopotential because the latter produces errors in the band gap and the dispersion of the energy bands. In Eq. (2) the integration over $\mathbf{k}$ space is performed numerically over an eight-dimensional cubic grid without factoring any of the terms from the integrand. The integration is performed over all regions of $\mathbf{k}$ space where the integrand is non-negligible. Auger transitions between the light- and heavy-hole valence bands and the bottom conduction band are included. For the *h-h-e* process the split-off valence band was used as well. Thus our results include all of the 27 different possible *h-h-e* transitions with holes 1, 2, and 2′ in the heavy-hole, light-hole, and split-off bands. Fermi-Dirac statistics are used to describe the occupation probabilities for the majority carriers [$f(E_1)$, $f(E_2)$, and $f(E_{2'})$] and Boltzmann statistics are used for the minority carriers [$f(E_{1'})$]. This corresponds to the physical conditions of the experiment[7] to which we compare our results. In the matrix element equation [Eq. (8)], all of the summations over the reciprocal lattice have been retained. The q dependence of the dielectric function is included in the form of Nara and Morita.[31] In our earlier work on AR in silicon[12,13] we used, in addition to the dielectric screening, a Thomas-Fermi screening factor, λ, for the free-electron screening. Since then, however, Burt[32] has pointed out that Thomas-Fermi screening is static, while the screening in Auger transitions is dynamic.[33] Since the frequencies in Auger transitions (1 eV) are much larger than the plasma frequency of the free carriers (0.1 eV), $\lambda=0$ is probably a better approximation. In this paper we present our results using $\lambda=0$. This results in Auger rates that are about 25% larger than those presented in our previous paper. This difference is of the order of the experimental errors of measurement, and does not affect any of our conclusions.

Because our calculations are a radical departure from previous work in the field, it is interesting to see which of the corrections that we have included are most significant. To this end we have checked some of the approximations that have appeared in previous Auger calculations by performing the same calculation (in silicon) both with and without each approximation. Of those tested, the two worst approximations are the neglect of the sum over the reciprocal lattice ("umklapp" terms), and the use of a static dielectric constant in the matrix elements. Each of these approximations decrease the total Auger transition rate by an order of magnitude. (Neglecting the dielectric screening altogether increases the rate by an order of magnitude.) These approximations may be better in the direct-band-gap materials, which have been the focus of much of the recent theoretical Auger work. Nonetheless, our results serve as a clear warning that such approximations should not be taken for granted, or buried in equations, as has often been done in the past. The use of Fermi-Dirac statistics (as opposed to Boltzmann statistics) increases the recombination rate when the carriers are degenerate. For example, at $T=77$ K, C_n increases by one-third between $n=10^{18}$ cm^{-3} and 10^{20} cm^{-3}. The effect of the statistics on C_p is even greater, because the effective density of states of the valence bands is lower than that of the conduction band. Because almost all of the previous Auger rate calculations use either $\mathbf{k}\cdot\mathbf{p}$ or parabolic band structures, we attempted to estimate the importance of accurate band structures. To this end we evaluate the Auger rate using parabolic bands (with the same effective masses as our pseudopotentials). Parabolic bands were used only in the evaluation of the energies in the statistical functions $f(E)$, [Eq. (2)]; the full band structure was used for the energy conservation condition. Nevertheless, the total Auger rate was off by 50%. We did not attempt to evaluate the influence of accurate wave functions on our results. Brand *et al.*[21] compared pseudopotential and 15 band $\mathbf{k}\cdot\mathbf{p}$ wave functions in their matrix-element formula and got similar results in either case. (Much of the previous Auger work, however, used only four band $\mathbf{k}\cdot\mathbf{p}$ wave functions, which are less accurate.)

We will now describe the method used to perform the $\mathbf{k}$-space integration [Eq. (2)]. The key to making the eight-dimensional surface integral tractable is to restrict our attention to those regions where the integrand is non-negligible. The occupation probability functions, $f(E)$, guarantee that these regions occur when $\mathbf{k}_1$, $\mathbf{k}_2$, and $\mathbf{k}_{1'}$ fall near their respective band edges. We have restricted the integration over $\mathbf{k}$ to those regions of $\mathbf{k}$-space satisfying $E_{\text{sum}}=(E_1-E_c)+(E_2-E_c)-(E_{1'}-E_v)\leq E_{\text{cut}}$ for *e-e-h* AR, and $E_{\text{sum}}=-(E_1-E_v)-(E_2-E_v)+(E_{1'}-E_c)\leq E_{\text{cut}}$ for *h-h-e* AR. This choice is based on the fact that the total occupation probability (using Boltzmann statistics) is proportional to $\exp(-E_{\text{sum}}/kT)$. The values of E_{cut} used in our calculations range from 200 to 350 meV, depending on the temperature. For silicon, which has an indirect band gap with the conduction-band minimum at $\mathbf{k}=0.85$ (all k vectors are units of $2\pi/A$, where A is the lattice constant), there are several different regions where the integrand is non-negligible. For *h-h-e* recombination there are six regions, in which $\mathbf{k}_1$ and $\mathbf{k}_2$ are holes near the center of the Brillouin Zone and $\mathbf{k}_{1'}$ is in the valley near one of the six conduction-band minima. Because all six regions are equivalent, the calculation for *h-h-e* recombination need be done for only one of the regions, and multiplied by 6. The situation for *e-e-h* recombination is more complicated; here there are three inequivalent types of regions. In the first type, $\mathbf{k}_1$ and $\mathbf{k}_2$ are the same conduction-band valley [for example $\mathbf{k}_1=\mathbf{k}_2=(0.85,0,0)$]. There are six regions of this type. In the second type, $\mathbf{k}_1$ and $\mathbf{k}_2$ are in orthogonal valleys [$\mathbf{k}_1=(0.85,0,0)$ and $\mathbf{k}_2=(0,0.85,0)$]. There are 12 regions of this type. In the third type, of which there are three regions, $\mathbf{k}_1$ and $\mathbf{k}_2$ are in opposite valleys [$\mathbf{k}_1=(0.85,0,0)$ and $\mathbf{k}_2=(-0.85,0,0)$]. The contributions to the Auger rate from the first two types of regions are about the same size. The contribution from the

third type of region is 2 orders of magnitude smaller than that of either of the first two, and is not included in any of the results presented here.

To produce the mesh for the **k**-space integration, a three-dimensional cubic mesh is generated for each of $\mathbf{k}_1$, $\mathbf{k}_2$, $\mathbf{k}_{1'}$, and $\mathbf{k}_{2'}$. The side of each cube has length Δk. The pseudopotential energies for the appropriate bands (three valence bands for holes, one conduction band for electrons) are evaluated at each grid point of the four meshes. The Cartesian product of these four meshes produces a twelve-dimensional mesh of the form $(\mathbf{k}_1,\mathbf{k}_2,\mathbf{k}_{1'},\mathbf{k}_{2'})$. Applying momentum conservation to fix $\mathbf{k}_{2'}$ reduces the mesh to nine dimensions $(\mathbf{k}_1,\mathbf{k}_2,\mathbf{k}_{1'},\mathbf{k}_1+\mathbf{k}_2-\mathbf{k}_{1'})$. The grid points form the vertices of a collection of 9 cubes in **k** space. The set of 9 cubes that intersect the energy-conservation surface $(E_1+E_2=E_{1'}-E_{2'})$ define a mesh over the surface. To determine whether a cube intersects the energy-conservation surface, $E_1+E_2-E_{1'}-E_{2'}$ is evaluated at the 512 vertices of each 9 cube; if this quantity crosses zero between any two vertices, then the cube is placed on a list of cubes that make up the final integration mesh. Next, we construct the wave functions that are needed for the evaluation of the matrix elements. The list of cubes that intersect the energy-conservation surface is used to find the grid points at which the wave functions are required. First, we shift the grids by $\Delta k/2$ in each dimension, so that the grid points now lie at the center of the cubes, rather than at the vertices. The pseudopotential wave function of a point in the $\mathbf{k}_1$ grid is evaluated if that value of $\mathbf{k}_1$ occurs as the first component of the coordinates $(\mathbf{k}_1,\mathbf{k}_2,\mathbf{k}_{1'},\mathbf{k}_{2'})$ of the center of one of the 9 cubes on the list. The same is done for $\mathbf{k}_2$, $\mathbf{k}_{1'}$, and $\mathbf{k}_{2'}$. Next the matrix elements are calculated at the center of each cube using Eq. (8) and the wave functions. The pseudopotential energies are used to evaluate the Fermi (or Boltzmann) functions. The advantage of using a cubic mesh is clear. The number of points in each dimension of the mesh is proportional to $N=1/\Delta k$. The number of cubes in the grid over the energy conservation surface (and thus the number of points at which the Auger matrix element need be calculated) is of order N^8: the number of points in each of the grids over $\mathbf{k}_1$, $\mathbf{k}_2$, $\mathbf{k}_{1'}$, and $\mathbf{k}_{2'}$, is proportional to N^3. Thus the total number of wave functions evaluated is about $4N^3$, which is much smaller than the N^8 matrix elements that they determine. In a typical calculation, we used fewer than 1 000 wave functions to calculate 300 000 matrix elements.

We performed careful convergence tests on all of the numerical cutoffs in our calculations. Each parameter was tested separately (with all other parameters held constant), and the tests were performed for all of the calculations (both *e-e-h* and *h-h-e* recombination and at all temperatures). We achieved convergence to within 1% in nearly all cases. (For some low temperature *h-h-e* results only 10% convergence was achieved.) Convergence tests were performed for the following numerical parameters: the number of plane waves used in the energy-band calculation; the number of reciprocal-lattice vectors used in the matrix-element sums; the size of the **k**-space mesh (Δk) used in the integration; the energy cutoff (E_{cut}).

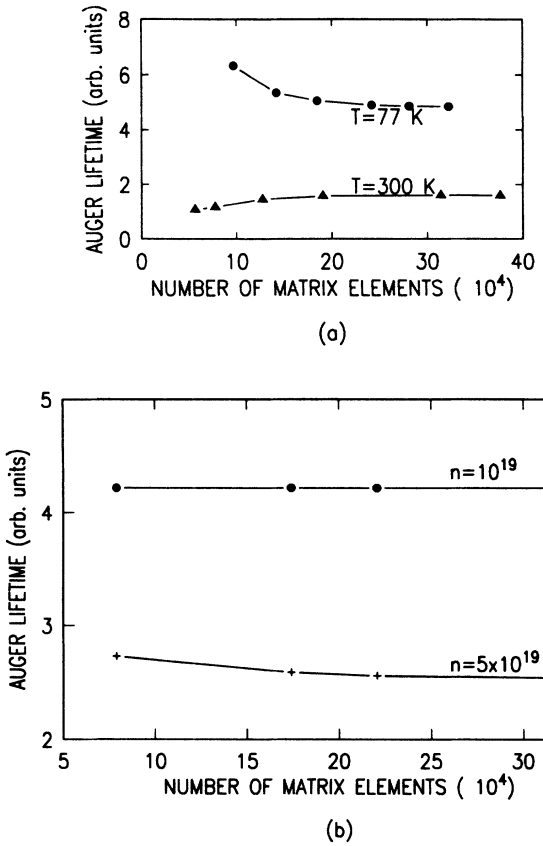

FIG. 3. (a) Convergence of the *e-e-h* Auger lifetime when the mesh size (Δk) is changed with all other parameters held constant. (b) Convergence of the *e-e-h* Auger lifetime when the energy cutoff (E_{cut}) is changed with all other parameters held constant.

Two of the convergence curves (for Δk and E_{cut}) are shown in Fig. 3.

RESULTS AND DISCUSSION

We compare our results (Fig. 4) with the experimental lifetimes of Dziewior and Schmid,[7] who measured the minority-carrier lifetimes in heavily doped *n*-type and *p*-type silicon. We chose this experiment for comparison, because it gives the simplest and most direct measurement of the Auger lifetimes. The authors also give separate lifetimes for both *e-e-h* and *h-h-e* AR, over a broad temperature range. (They also measure the Auger rate at $T=4$ K, but we did not extend our calculations to such low temperatures.) A more complex experiment by Svantesson and Nilsson[8] produced very similar results for highly excited intrinsic silicon.

The differences between our results for *e-e-h* and *h-h-e* AR are striking. For *e-e-h* recombination, the theoretical and experimental lifetimes are in very good agreement at both high and low temperatures. For *h-h-e* recombination, in contrast, the theoretical lifetimes are an order of magnitude slower than the experimental values, at best.

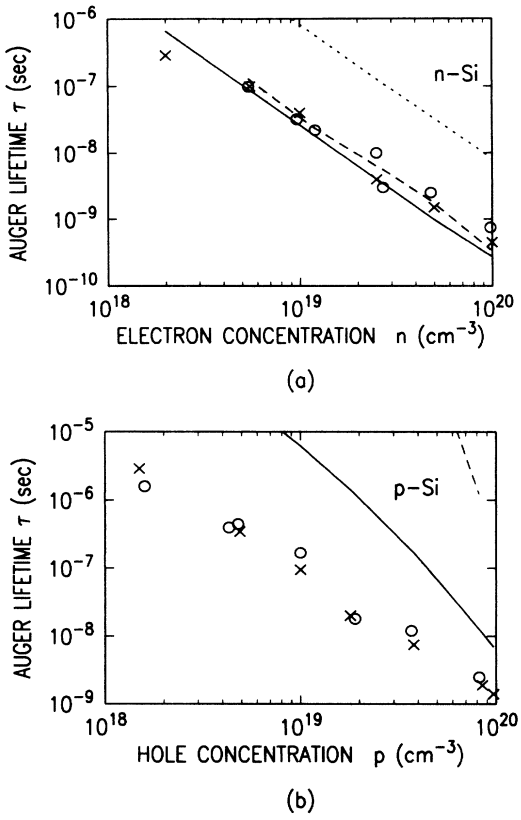

FIG. 4. Experimental and theoretical Auger lifetimes. Experimental results of Dziewior and Schmid (Ref. 7) indicated by circles ($T=77$ K), and X's ($T=300$ K). Theoretical results indicated by dashed ($T=77$ K) and solid lines ($T=300$ K). For comparison, the theoretical results of Hill and Landsberg (Ref. 6) (for n-type Si) are indicated by a dotted line ($T=300$ K).

The temperature dependence of the theoretical rates differs as well. While the *e-e-h* rates are nearly temperature independent, the *h-h-e* rates increase rapidly with temperature. The experimental rates show a very weak temperature dependence for both *e-e-h* and *h-h-e* AR. Our pure AR results account for the observed lifetimes in n-type silicon but not in p-type silicon.

These results are consistent with the assertion of Huldt[5] that pure *e-e-h* Auger transitions are much more probable than pure *h-h-e* transitions. Huldt's theoretical *e-e-h* rate is, however, an order of magnitude smaller than experiment. Later calculations by Hill and Landsberg[6] produced similar results. The authors cautioned, however, that because of the uncertainties in the calculations, their rates were not definitive. These theoretical results led to the conclusion that phonon-assisted Auger recombination dominates in both n-type and p-type silicon. The weak temperature dependence of the Auger lifetimes was cited as additional evidence of the role of phonon-assisted processes; Haug[9] found that this temperature dependence could be fitted by phonon-assisted mechanism (where the temperature enters through the statistical probability of phonon emission), but not by a pure AR mechanism (where the temperature enters through the occupation probabilities of the electrons; see below). When Lochmann and Haug[11] calculated the phonon-assisted Auger rate for both *e-e-h* and *h-h-e* transitions, they obtained good agreement for *h-h-e* AR, but their results for *e-e-h* recombination were still four times smaller than the experimental values. The point we wish to emphasize here is that the assertion that pure AR is not important in silicon rests entirely on the results of prior theory. But our work shows that, in an accurate theory, both the magnitude and the temperature dependence of the pure *e-e-h* rate agree very well with experiment. We now reopen the question of which recombination mechanism dominates in silicon, pure or phonon-assisted AR? In prior theory the phonon-assisted rates are faster, but both the pure and phonon-assisted calculations used approximations that we have already demonstrated to be invalid. Besides, the theoretical values for the pure and phonon-assisted mechanisms were obtained using different approximations. In particular, the phonon-assisted Auger recombination rate calculation[11] does not include dielectric screening ($\epsilon=1$), while the pure Auger rate calculations[5,6] use static dielectric screening ($\epsilon=12$). Because the Auger rate depends on ϵ^{-2}, using the same ϵ in both theories would give a pure Auger rate an order of magnitude larger than the phonon-assisted rate. To our knowledge, no one has calculated both pure and phonon-assisted AR rates using consistent approximations. Ideally, we should answer this question by calculating the phonon-assisted AR rates in silicon to the same degree of accuracy as our pure AR calculation, but accurate phonon-assisted rates, which involve an additional integration over phonon momenta, are beyond the limits of present computational capabilities. Instead we present a physical argument to explain why pure AR should dominate in n-type silicon, and phonon-assisted AR in p-type silicon.

The key to understanding the differences between *e-e-h* and *h-h-e* AR and the relation of pure AR to phonon-assisted AR lies in the concept of recombination thresholds. The thresholds are a consequence of the energy- and momentum-conservation conditions that must be satisfied by the initial and final electronic states. As mentioned above, these conditions determine an eight-dimensional surface in $\mathbf{k}$ space, and Auger transitions can occur only for configurations that lie on this surface. The largest contributions to the Auger rate are those for which $\mathbf{k}_1$, $\mathbf{k}_2$, and $\mathbf{K}_{1'}$ are nearest to their respective band edges: otherwise, the statistical function $f(E_1)f(E_2)[1-f(E_{1'})]$ will be vanishingly small. $f(E_1)f(E_2)[(1-f(E_{1'})]$ obtains its maximum value for the configuration that has $\mathbf{k}_1$, $\mathbf{k}_2$, and $\mathbf{k}_{1'}$ at the band edges, but the energy-conservation surface need not contain this configuration. The recombination threshold is the configuration on the energy conservation surface that has the maximum value of $f(E_1)f(E_2)[1-f(E_{1'})]$. Using Boltzmann statistics for $f(E)$, we have

$$f(E_1)f(E_2)[1-f(E_{1'})] = \frac{n^2p}{N_c^2N_v}e^{[-(E_1-E_c)-(E_2-E_c)+(E_{1'}-E_v)]/kT}$$

for *e-e-h* AR, and

$$f(E_1)f(E_2)[1-f(E_{1'})] = \frac{np^2}{N_c N_v^2} e^{[(E_1-E_{v'})+(E_2-E_{v'})-(E_{1'}-E_c)]/kT}$$

for *h-h-e* AR. (Note that the statistical functions introduce, besides the explicit exponential dependence, a $T^{-9/2}$ dependence through the presence of N_c and N_v.) In either case, $f(E_1)f(E_2)[1-f(E_{1'})]$ is proportional to $\exp(-E_{\text{sum}}/kT)$. (E_{sum} is defined in the previous section.) Thus, when Boltzmann statistics is applicable, the threshold configuration is simply the configuration that has the minimum value of E_{sum}. We call this configuration the Boltzmann threshold configuration. The threshold energy, E_{Th}, is defined as this minimum value of $E_{\text{sum}}[E_{\text{Th}}=E_{\text{sum}}(\mathbf{k}_{\text{Th}})$, where $\mathbf{k}_{\text{Th}}$ is the threshold configuration]. When Fermi-Dirac statistics applies, $f(E_1)f(E_2)[1-f(E_{1'})]$ will not, in general, achieve its maximum value at the minimum value of E_{sum}. Here the threshold configuration will depend on the carrier concentrations, and a threshold energy cannot be defined. Nonetheless, if the carriers are not strongly degenerate, the difference between the two configurations will be small. We will assume that this condition holds, and will use the Boltzmann threshold configuration in our discussions. (This approximation does not enter our calculations, where we use Fermi-Dirac statistics and calculate the Auger rates without direct reference to the threshold.)

Because the total Auger rate is very sensitive to the value of E_{Th}, the relative importance of pure and phonon-assisted AR depends on the difference in thresholds between the two processes. Huldt[5] estimated that for *e-e-h* recombination in silicon $0 \le E_{\text{Th}} \le 52$ meV, but that the *h-h-e* recombination threshold was so large that phonon-assisted recombination was likely to dominate. In the work of both Huldt and of Hill and Landsberg,[6] a threshold of zero was used for calculation of the pure *e-e-h* rate. If the threshold is in fact zero, it is unlikely that phonon-assisted recombination, a *second-order* process, dominates over pure *e-e-h* recombination, a *first-order* process. Although accurate thresholds are crucial to determining the dominant mechanism, there are no other theoretical investigations of the threshold for pure AR in silicon. We have evaluated E_{Th} for both *e-e-h* and *h-h-e* recombination as the minimum value of E_{sum} for all of the transitions included in our calculations. We find thresholds of 8 meV for *e-e-h* AR and 76 meV for *h-h-e* AR. Inspection of the band structure of silicon confirms that is easy to find *e-e-h* transitions near the band edge [Fig. 5(a)] but not *h-h-e* transitions [Fig. 5(b)]. (The figures show Auger transitions in which the **k** vectors are all restricted to a single dimension. In our evaluation of E_{Th} we have included **k** vectors in all dimensions.) These thresholds explain why the theoretical *e-e-h* rate is far larger than the *h-h-e* rate, and why the theoretical *h-h-e* rates have a much stronger temperature dependence than the *e-e-h* rates. We can also understand why phonon-assisted AR dominates in *p*-type silicon, and pure AR in *n*-type silicon. For *h-h-e* AR, where the pure Auger mechanism has a high threshold, a phonon-assisted process, even though it is second order, can compete by reducing the threshold. For *e-e-h* AR, where the pure AR threshold is already very low, there is no advantage for phonon-assisted recombination.

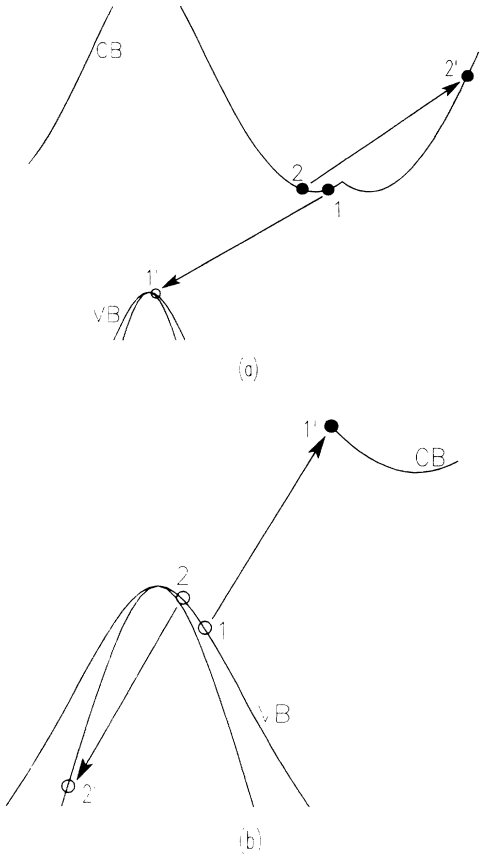

FIG. 5. (a) A possible *e-e-h* transition for silicon. (The top three valence bands and the one lowest conduction band are shown in the ⟨100⟩ direction, using a repeated zone scheme. The apparent cusp in the conduction band is caused by a band crossing at the *X* point.) (b) A possible *h-h-e* Auger transition.

One experiment was conducted to test which type of AR dominates in *n*-type silicon. It was claimed that the results demonstrate that phonon-assisted AR dominates; in fact, the results are inconclusive. Abakumov and Yassievich[34] examined theoretically the effect of uniaxial stress on the AR rate in silicon. If unaxial stress is applied along one of the ⟨100⟩ axes of the crystal, the two conduction-band minima along the stressed axis will be lowered with respect to the four other conduction-band minima. As a result, conduction electrons move from the other valleys to the two valleys that lie along the stressed axis. If enough pressure is applied, these two valleys will eventually contain all of the conduction electrons in the crystal, tripling their population. Abakumov and Yassievich assume that pure Auger transitions can occur only between electrons in the same conduction-band valley. With this assumption they conclude that the application

of uniaxial pressure should triple the pure Auger rate. Subsequently, Grekhov and Delimova[35] measured the experimental pressure dependence of the AR rate in silicon at room temperature. They found the recombination rate to be independent of applied pressure, even when the pressure-induced difference in the conduction-band minima was 40 meV. They concluded that the observed recombination is phonon assisted. (The authors claim that the phonon-assisted transition rate is not affected by uniaxial stress.) The crucial point in this analysis is the assumption that pure AR can only occur between electrons in the same conduction-band valley. Our calculations disprove this assumption; at room temperature the largest contribution to the pure Auger rate comes from the transitions involving electrons in the orthogonal valleys. We have repeated the analysis of Abakumov and Yassievich using the two components of C_n (for electrons in the same and in orthogonal valleys) from our calculation in place of the single Auger coefficient (for electrons in the same valley) used by Abakumov and Yassievich. We find that—even in the case when all of the electrons are transferred to the two preferred valleys—the rate of pure AR is increased by only 25%, which is within the range of experimental uncertainty. In addition, the pressure-induced change in the band structure has an unknown effect on the pure Auger rate, and may well offset the increase caused by the redistribution of the electrons. Also, it has not been demonstrated that the phonon-assisted Auger is independent of applied pressure. We maintain that, because of these arguments, the results of this experiment are inconclusive.

One further point to be explained is the behavior of the Auger coefficients at lower carrier concentrations. The experimental signature of AR is the carrier dependence of the Auger lifetimes, $\tau^{-1}=C_n n^2$ for *e-e-h* AR, or $C_p p^2$ for *h-h-e* AR. For heavily doped *n*-type Si, the Auger coefficient, C_n is constant at 2.7×10^{-31} cm^6 sec^{-1} when n is above 5×10^{18} cm^{-3}, but jumps suddenly to about 2×10^{-30} cm^6 sec^{-1} when n is below this value.[36–38] The behavior of C_p is similar. (According to Yablonovitch and Gmitter,[38] the carrier dependence of the *e-e-h* Auger rate is best described by an $n^{1.65}$ law, which has been explained either by equilibrium population effects,[39] or by a combination of band-to-band and trap-Auger recombination.[40]) Our calculations for *n*-type Si correctly predict the high-density Auger rates, but not the sudden increase of C_n below 5×10^{18} cm^{-3}. The dramatic change in the Auger coefficient is hard to explain. One possible explanation is that degeneracy reduces the Auger rate at high carrier concentrations. But the effects of degeneracy should be minimal at $n=5\times10^{18}$ cm^{-3} and should be more noticeable in the $n=10^{19}$ cm^{-3} to 10^{20} cm^{-3} range, where, in fact C_n is constant. Our calculations show that Fermi-Dirac statistics causes only a minor change in C_n even at $n=10^{20}$ cm^{-3}, and that it increases the recombination rate. Another possible explanation is that the effects of heavy doping on the band structure diminish the rate of AR. This can be ruled out because experimental measurements of C_n produce the same results in highly excited intrinsic silicon[8] as in heavily doped material.[7]

A more likely explanation of the experimental results is that the Auger rate is not reduced when n is large, but enhanced when n is small. The enhancement of the recombination rate can come from two sources: excitonic AR and AR through electrons in shallow levels. In either case the enhancement would end when the material undergoes a phase transition (caused by increased carrier screening). The abrupt nature of the change suggests that a phase transition is in fact present; the effects of degeneracy, band-structure shifts, and the like, should produce a gradual change that becomes more marked as n increases. Excitonic Auger processes involving actual excitons have been investigated theoretically by Hangleiter,[16,17] and Auger transition enhancement by electron-hole plasma interactions by Takeshima.[15] The increase in the Auger rate predicted by either of these papers is enough to account for the observed change in C_n. The excitonic Auger mechanism would be suppressed at higher carrier concentrations, where electron screening would be large enough to nullify the electron-hole attraction. The other possible source of enhancement is AR through donor electrons in shallow levels (or holes in acceptor states for *h-h-e* recombination). These electrons have localized wave functions that are spread over a much larger region of **k** space than the thermal distribution of conduction-band electrons. Bound electron AR, in combination with pure AR, would dominate below the metal-insulator transition, where there are bound-electron states available. Above the metal-insulator transition these bound states disappear and only pure Auger transitions can occur. Indeed, the change in the Auger coefficient occurs almost exactly at the metal-insulator transition in both *n*-type and *p*-type silicon.

In summary, we have presented an accurate method of calculating pure Auger recombination rates in semiconductors. Applying this method to silicon produces very good agreement with the experimental lifetimes in *n*-type material. We conclude that pure AR dominates in *n*-type silicon and phonon-assisted recombination dominates in *p*-type silicon. Our calculations also show that many of the approximations that have become standard in Auger theory are unreliable. We address the question of the sudden increase in the Auger coefficients below $n=5\times10^{18}$ cm^{-3}, and suggest that it is caused by either excitonic or bound-electron AR.

ACKNOWLEDGMENTS

We are grateful to M. G. Burt (British Telecom, Ipswich, United Kingdom), A. Hangleiter (Universitat Stuttgart, Stuttgart, Germany), and E. Yablonovitch (Bell Communications Research, Red Bank, NJ), for valuable discussions. One of us (D.B.L.) acknowledges support from IBM. This work was supported in part by U.S. Office of Naval Research (ONR) Contract No. N00014-84-C-0396 and a New York State Center for Advanced Technology (CAT) Program Grant to Columbia University.

[1]A. R. Beattie and P. T. Landsberg, Proc. R. Soc. London Ser. A **249**, 16 (1958).
[2]P. T. Landsberg, Solid State Electron. **30**, 1107 (1987).
[3]M. Takeshima, J. Appl. Phys. **58**, 3846 (1985).
[4]M. A. Green, IEEE Trans. Electron Devices **ED-31**, 671 (1984).
[5]L. Huldt, Phys. Status Solidi A **8**, 173 (1971).
[6]D. Hill and P. T. Landsberg, Proc. R. Soc. London Ser. **347**, 547 (1976).
[7]J. Dziewior and W. Schmid, Appl. Phys. Lett. **31**, 346 (1977).
[8]K. G. Svantesson and N. G. Nilsson, J. Phys. **12**, 5111 (1979).
[9]A. Haug, Solid State Commun. **28**, 291 (1978).
[10]A. Haug and W. Schmid, Solid State Electron. **25**, 665 (1978).
[11]W. Lochmann and A. Haug, Solid State Commun. **35**, 553 (1980).
[12]D. B. Laks, G. F. Neumark, A. Hangleiter, and S. T. Pantelides, Phys. Rev. Lett. **61**, 1229 (1988).
[13]D. B. Laks, G. F. Neumark, A. Hangleiter, and S. T. Pantelides, in *Shallow Impurities in Semiconductors 1988,* Inst. Phys. Conf. Ser. 95, edited by B. Monemar (Institute of Physics, Bristol, 1989), p. 515.
[14]A. M. Stoneham, *Theory of Defects in Solids* (Oxford University Press, London, 1975), p. 539.
[15]M. Takeshima, Phys. Rev. B **28**, 2039 (1983).
[16]A. Hangleiter and R. Hacker, in *Proceedings of the Eighteenth International Conference on the Physics of Semiconductors,* edited by O. Engström (World Scientific, Singapore, 1987), p. 907.
[17]A. Hangleiter, Phys. Rev. B **37**, 2594 (1988).
[18]B. K. Ridley, *Quantum Processes in Semiconductors* (Clarendon, Oxford, 1982), p. 268.
[19]J. Callaway, *Quantum Theory of the Solid State* (Academic, New York, 1974), p. 585.
[20]The frequency dependence of ϵ is not included because it is not important in homopolar semiconductors like silicon.
[21]S. Brand and R. A. Abram, J. Phys. C **17**, L201 (1984).
[22]S. Brand and R. A. Abram, J. Phys. C **17**, L571 (1984).
[23]M. G. Burt, S. Brand, C. Smith, and R. A. Abram, J. Phys. C **17**, 6385 (1984).
[24]M. G. Burt and C. Smith, J. Phys. **17**, L47 (1984).
[25]W. Bardyszewski and D. Yevick, J. Appl. Phys. **57**, 4820 (1985).
[26]W. Bardyszewski and D. Yevick, J. Appl. Phys. **58**, 2713 (1985).
[27]L. Huldt, N. G. Nilsson, and K. G. Svantesson, Appl Phys. Lett. **35**, 776 (1979).
[28]P. Scharoch and R. A. Abram, Semicond. Sci. Technol. **3**, 973 (1988).
[29]A. R. Beattie, J. Phys. C **18**, 6501 (1985).
[30]J. R. Chelikowsky and M. L. Cohen, Phys. Rev. B **10**, 5095 (1974).
[31]H. Nara and A. Morita, J. Phys. Soc. Jpn. **21**, 1852 (1966).
[32]M. G. Burt (private communication).
[33]M. G. Burt, J. Phys. C **14**, 3269 (1981).
[34]V. N. Abakumov and I. N. Yassievich, Fiz. Tekh. Poluprovodn. **11**, 1302 (1977) [Sov. Phys.—Semicond. **11**, 766 (1977)].
[35]I. V. Grekhov and L. A. Delimova, Fiz. Tekh. Poluprovodn. **14**, 897 (1980) [Sov. Phys.—Semicond. **14**, 529 (1980)].
[36]Yu Vaitkus and V. Grivitiskas, Fiz. Tekh. Poluprovodn. **15**, 1894 (1981) [Sov. Phys.—Semicond. **15**, 1102 (1981)].
[37]J. G. Fossum, R. P. Mertens, D. S. Lee, and J. F. Nijs, Solid State Electron. **26**, 569 (1983).
[38]E. Yablonovitch and T. Gmitter, Appl. Phys. Lett. **49**, 587 (1986).
[39]A. Haug, J. Phys. C **21**, L287 (1988).
[40]P. T. Landsberg, Appl. Phys. Lett. **50**, 745 (1987).